

# Diffuse microvascular dysfunction and loss of white matter integrity predict poor outcomes in patients with acute ischemic stroke

Natalia S Rost<sup>1</sup>, Pedro Cougo<sup>1</sup>, Svetlana Lorenzano<sup>1,2</sup>, Hua Li<sup>1,3</sup>, Lisa Cloonan<sup>1</sup>, Mark JRJ Bouts<sup>1,4</sup>, Arne Lauer<sup>1</sup>, Mark R Etherton<sup>1</sup>, Hasan H Karadeli<sup>1</sup>, Patricia L Musolino<sup>1</sup>, William A Copen<sup>3</sup>, Ken Arai<sup>5</sup>, Eng H Lo<sup>5</sup>, Steve K Feske<sup>6</sup>, Karen L Furie<sup>7</sup> and Ona Wu<sup>1,3,4</sup>

## Abstract

We sought to investigate the relationship between blood–brain barrier (BBB) permeability and microstructural white matter integrity, and their potential impact on long-term functional outcomes in patients with acute ischemic stroke (AIS). We studied 184 AIS subjects with perfusion-weighted MRI (PWI) performed <9 h from last known well time. White matter hyperintensity (WMH), acute infarct, and PWI-derived mean transit time lesion volumes were calculated. Mean BBB leakage rates (K<sub>2</sub> coefficient) and mean diffusivity values were measured in contralesional normal-appearing white matter (NAWM). Plasma matrix metalloproteinase-2 (MMP-2) levels were studied at baseline and 48 h. Admission stroke severity was evaluated using the NIH Stroke Scale (NIHSS). Modified Rankin Scale (mRS) was obtained at 90-days post-stroke. We found that higher mean K<sub>2</sub> and diffusivity values correlated with age, elevated baseline MMP-2 levels, greater NIHSS and worse 90-day mRS (all  $p < 0.05$ ). In multivariable analysis, WMH volume was associated with mean K<sub>2</sub> ( $p = 0.0007$ ) and diffusivity ( $p = 0.006$ ) values in contralesional NAWM. In summary, WMH severity measured on brain MRI of AIS patients is associated with metrics of increased BBB permeability and abnormal white matter microstructural integrity. In future studies, these MRI markers of diffuse cerebral microvascular dysfunction may improve prediction of cerebral tissue infarction and functional post-stroke outcomes.

## Keywords

White matter lesions, acute ischemic stroke, blood–brain barrier, matrix metalloproteinase-2, outcomes

Received 19 October 2016; Revised 7 February 2017; Accepted 20 March 2017

## Introduction

Diffuse cerebral small vessel disease detected on T2-weighted MRI as white matter hyperintensity (WMH) or leukoaraiosis is a common finding that is strongly linked to functional decline in aging adults and to poor stroke outcomes.<sup>1–3</sup> Although risk factors such

<sup>4</sup>Athinoula A. Martinos Center for Biomedical Imaging, Massachusetts General Hospital and Harvard Medical School, Charlestown, MA, USA

<sup>5</sup>Neuroprotection Research Laboratory, Neuroscience Center, Departments of Neurology and Radiology, Massachusetts General Hospital and Harvard Medical School, Charlestown, MA, USA

<sup>6</sup>Department of Neurology, Brigham and Women's Hospital, Boston, MA, USA

<sup>7</sup>Department of Neurology, Rhode Island Hospital, Providence, RI, USA

### Corresponding author:

Natalia S Rost, MPH J. Philip Kistler Stroke Research Center, Massachusetts General Hospital, 175 Cambridge Street, Suite 300, Boston, MA 02114, USA.  
Email: nrost@partners.org

<sup>1</sup>J. Philip Kistler Stroke Research Center, Department of Neurology, Massachusetts General Hospital and Harvard Medical School, Boston, MA, USA

<sup>2</sup>Department of Neurology and Psychiatry, Sapienza University of Rome, Rome, Italy

<sup>3</sup>Department of Radiology, Massachusetts General Hospital and Harvard Medical School, Boston, MA, USA

as advanced age, hypertension, hyperhomocysteinemia, and smoking have been associated with WMH, variability in WMH severity is largely unexplained, and its pathophysiology remains elusive.<sup>4</sup> Chronic hypoperfusion has been proposed as one underlying mechanism of WMH progression, as subcortical white matter is characterized by regions of terminal circulation with poor or absent collateral flow, and patients with increased WMH burden have impaired cerebrovascular reactivity and reduced periventricular cerebral blood flow (CBF).<sup>5–7</sup>

Another hypothesis is that vascular risk factors may induce progressive chronic endothelial injury, disrupting the blood–brain barrier (BBB) and leading to parenchymal accumulation of blood constituents that are potentially neurotoxic.<sup>8,9</sup> One potential mechanism implicated in this process is linked to matrix metalloproteinase-2 (MMP-2), an enzyme known for its role in chronic BBB remodeling, which is activated by hypoxia-inducible factor 1 (HIF-1) early during an acute cerebral ischemic event.<sup>10,11</sup> Prior studies have shown that WMH volume (WMHv) is associated with circulating plasma MMP-2 levels in patients with acute ischemic stroke (AIS);<sup>12</sup> however, it is not clear whether the elevated MMP-2 levels directly translate to detectable BBB disruption. One radiographic approach to evaluate microvascular BBB disruption is to measure the effects of leakage of contrast agent (i.e., “K2 coefficient”) to extravascular space.<sup>13</sup>

If the association between BBB integrity, circulating MMP-2 levels, and WMH severity is confirmed, this study may suggest a plausible underlying biological mechanism that links WMH burden and BBB permeability. Because changes in diffusivity of water molecules have been suggested to be precursors of eventual WMH development on FLAIR,<sup>14</sup> we will also investigate the association between BBB permeability and diffusivity.

To test the hypothesis that WMH severity is associated with increasing BBB permeability, as a measure of diffuse microvascular dysfunction, and that circulating levels of MMP-2 are correlated with the MRI markers of white matter structural integrity, we sought to: (1) examine the relationship between BBB permeability and microstructural white matter integrity in normal-appearing white matter (NAWM), as measured by K2 coefficients and apparent diffusivity coefficients (ADC), respectively, and (2) investigate their association with degree of acute cerebral tissue injury and long-term functional outcomes.

## Materials and methods

### Subjects

The study was approved by the Partners Human Research Committee (protocol # 2011P002725), which

operates in compliance with all applicable regulations and guidelines pertaining to Institutional Review Boards as follows: Department of Health and Human Services (DHHS) 45 CFR Parts 46 and 164, Food and Drug Administration (FDA) 21 CFR Parts 50 and 56 and International Conference on Harmonization (ICH) guidance relating to Good Clinical Practice (GCP), section 3 (3.1–3.4) unless ICH guidelines conflict with FDA Regulations. All participating subjects or their surrogates provided informed consent. We retrospectively analyzed data from a prospective cohort of consecutive adult (age  $\geq 18$  years) AIS patients admitted to our institution from February 2007 to February 2011 as part of an observational NIH Specialized Program of Translational Research in Acute Stroke (SPOTRIAS) study.<sup>12</sup>

All patients presenting to two participating academic medical centers within 9 h of last known well (LKW) time were eligible. For all consented subjects, data were acquired through medical record review or in-person interviews. Baseline clinical characteristics were obtained on admission. For this study, patients were included if they met the following criteria: (a) MRI performed at admission ( $< 9$  h from LKW) that included diffusion-weighted MRI (DWI), dynamic susceptibility contrast-enhanced (DSC) perfusion-weighted MRI (PWI), and T2-weighted fluid-attenuated inversion recovery (FLAIR) MRI; (b) evidence of a confirmed acute infarct on DWI; and (c) plasma MMP-2 levels collected at the time of enrollment.

### Matrix metalloproteinase-2 analysis

Plasma samples were collected twice: in the acute phase (less than 9 h after stroke onset) and at 48 h (36–60 h after stroke onset). Samples were drawn in ethylenediaminetetraacetic acid tubes, using a butterfly needle to reduce shear stress, placed on ice and immediately centrifuged at 3000 revolutions per minutes for 15 min. Plasma was subsequently isolated and frozen at  $-80^{\circ}\text{C}$  for later measurement. Levels of MMP-2 were analyzed using a commercially available enzyme-linked immunosorbent assay (ELISA) (R&D systems) and expressed in nanograms per milliliter (ng/mL). ELISA was performed according to the manufacturer’s instructions by investigators (K.A., E.H.L.) blinded to clinical and imaging information.

### Imaging analysis

**MRI data acquisition.** All MRI was performed on 1.5T General Electric scanners with the exception of three studies that were acquired on a 3T Siemens system. For 10 cases, FLAIR scans were acquired on a different scan date from the DWI and PWI scans due to

unusable or unavailable FLAIR scans. For the majority of the subjects, axial T2-weighted FLAIR MRI was acquired with TR/TE/TI = 10002/145/2200 ms, 220 mm field-of-view (FOV), 5 mm slice thickness with 1 mm gap, and in-plane resolution of  $0.86 \times 0.86 \text{ mm}^2$ .

Diffusion tensor imaging (DTI) was acquired using echo-planar imaging (EPI) with the following parameters for the majority of the cases: TR/TE = 5000/85.3 ms, 220 mm FOV, 5-mm slice thickness with 1-mm gap, in-plane resolution of  $0.86 \times 0.86 \text{ mm}^2$  ( $128 \times 128$  acquisition matrix up-sampled to  $256 \times 256$ ), three  $0 \text{ s/mm}^2$  (b-zero) and  $1000 \text{ s/mm}^2$  b-values in 25 directions. DTI datasets were corrected for motion and eddy current distortions.<sup>15</sup> ADC maps were derived mathematically from the high- and low-b-value images.<sup>15</sup>

PWI was performed using serial acquisition of gradient-echo EPI T2\*-weighted images. Images were acquired before and during power injection of a gadolinium-based contrast agent. The imaging protocol consisted of 80 acquisitions at a TR/TE = 1500/40 ms, 220 mm FOV, 5 mm slice thickness with 1 mm gap,  $1.72 \times 1.72 \text{ mm}^2$  in plane resolution for most of the cases. K2 coefficients ( $s^{-1}$ ) were derived from the concentration-time curves using the Boxerman-Weisskoff model and techniques previously described.<sup>13</sup> In brief, the measured concentration-time curve can be modeled as

$$\Delta \bar{R}_2^*(t) \approx K_1 \overline{\Delta R_2^*(t)} - K_2 \int_0^t \overline{\Delta R_2^*(t')} dt'$$

where  $\Delta R_2^*(t)$  is the true concentration, and solve for  $K_2$  using a linear least-squares fit.

Cerebral blood volume (CBV), CBF, and mean transit time (MTT) maps were calculated from DSC data that were converted to concentration changes over time curves and deconvolved with an automatically selected arterial input function.<sup>16,17</sup>

**Volumetric image analysis.** WMH lesions were outlined using MRICro software (*University of Nottingham School of Psychology, Nottingham, UK; www.mricro.com*). Experienced operators blinded to K2 results outlined the WMH region on each supratentorial FLAIR slice and saved the outline as a region of interest (ROI). Another whole-brain WMH ROI was created by setting a threshold that matched the supratentorial WMH ROI intensity. The intersection between these two ROIs was manually edited to produce the final WMH ROI, and WMHv was generated for each subject. To reduce confounds from hyperintensity due to acute infarction, analysis was limited to the contralesional hemisphere. Scans with bilateral acute infarcts were excluded from analysis. DWI and FLAIR sequences were

cross-referenced to ensure the exclusion of T2-hyperintense signal due to edema, chronic infarcts, or acute ischemia.

Volumes of perfusion deficits measured on ipsilateral MTT maps (MTTv) and DWI lesion volumes (DWIv) were calculated semi-automatically, using MRICro software. Intensity threshold-based method used for WMHv calculation (see above) was adopted for the purpose of DWIv and MTTv calculation. ADC maps were cross-referenced against DWI maps to ensure exclusion of subacute and chronic T2-hyperintense lesions. All images were analyzed by trained research staff (S.L., H.L., L.C., A.L., H.H.K., M.R.E., N.S.R.), each of whom received standardized instruction and tested against a “gold standard” set (n = 10) with inter-rater correlation coefficient 0.92–0.95 prior to deriving volumetric data for this dataset. All readers were blinded to K2 results, clinical characteristics, and outcome data.

**Normal-appearing white matter analysis.** DWI, PWI and FLAIR datasets were co-registered to one another using semi-automated co-registration software (MNI Autoreg<sup>18</sup>) and to the ICBM-452 T1 5th Order Polynomial Warps Atlas.<sup>19</sup> Using the ICBM probabilistic atlas,<sup>20,21</sup> white matter masks were created using a threshold of 95% probability. NAWM was segmented from the hemisphere contralateral to the acute infarct by subtracting the WMH ROI from white matter masks. To minimize inclusion of abnormal tissue in NAWM masks, the WMH ROIs were first dilated successively three times (mincmorph<sup>22</sup>) prior to subtraction, and NAWM masks limited to tissue with ADC values less than  $1200 \times 10^{-6} \text{ mm}^2/\text{s}$  (Figure 1). The mean K2 coefficients and ADC were measured in the NAWM.

### Outcome definitions

Functional outcome was measured as modified Rankin scale score (mRS) at 90 days after AIS, obtained either by in-person interview, or using a validated telephone-based approach.<sup>23</sup> Outcome was considered favorable in patients with 90-day mRS < 2.

Hemorrhagic transformation (HT) was defined as presence of hemorrhagic infarction (petechial hemorrhage) or parenchymal hematoma on imaging completed within 48 h of LKW (T2\* MRI sequence, or non-contrast head CT) based on European Collaborative Acute Stroke Study (ECASS) criteria.<sup>24</sup>

### Statistical analysis

All variables were reported as either a mean value ( $\pm$ standard deviation [SD]), a median value with an

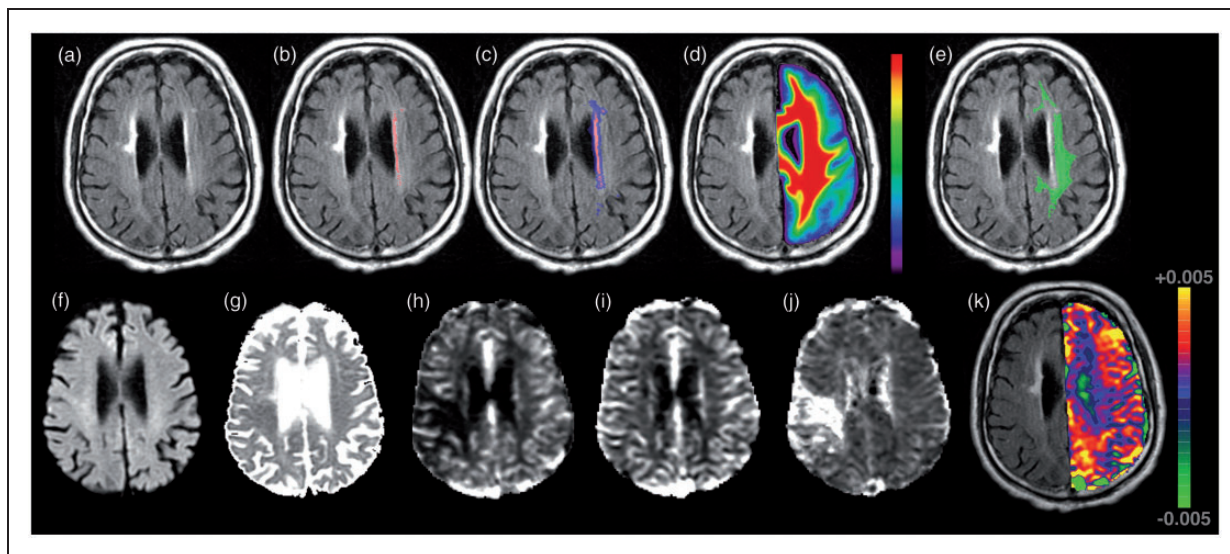


**Figure 1.** Neuroimaging characteristics of diffuse microvascular dysfunction in a patient with acute ischemic stroke. *Top row* (panel a–e) demonstrates an example of the normal-appearing white matter region-of-interest in a patient with acute ischemic stroke and white matter hyperintensity volume of 2.36 cm<sup>3</sup>. (a) FLAIR image, (b) manual WMH outline (red), (c) dilated WMH outline (blue + red), (d) co-registered white matter probability mask, (e) contralateral normal appearing white matter mask (green) calculated as voxels with probability >95% of being white matter AND not in dilated mask (c). *Bottom row* (panel f–k) demonstrates this patient's acute (f) DWI, (g) ADC, (h) CBF, (i) CBV, (j) MTT, and (k) K2 map shown overlaid on the FLAIR scan (for clarity only the contralateral hemisphere values are shown). All images are displayed in radiologic format.

interquartile range (IQR), or a proportion/percentage of total. Lesion volumes and MMP-2 values were log-transformed for all regression analyses. Univariable analysis was performed using Wilcoxon two-sample rank sum test for nominal variables, Spearman's correlation coefficient for ordinal or continuous variables and logistic regression for binary responses, as appropriate. Variables that showed a *P*-value of <0.10 in univariable analysis were used in multivariable linear regression implemented with backward stepwise regression. The selected variables to include in the final model are based on the Akaike Information Criterion (AIC), a measure that is a function of both training error and complexity.<sup>25</sup> Statistical analyses were performed using JMP Pro 12.2.0 (SAS Institute, Middleton, MA).

## Results

One hundred eighty-four AIS subjects met our inclusion criteria (Table 1). Sixty-five patients (35%) received thrombolytic treatment, of which 64 patients received intravenous tissue plasminogen activator (IV tPA) only, and 1 patient underwent combined treatment (IV tPA plus intra-arterial treatment). Patients treated with thrombolytic therapy (N = 65) exhibited significantly larger acute DWI volumes (13.2 [2.5–37.8] cm<sup>3</sup> vs. 5.7 [1.2–18.9 cm<sup>3</sup>]; *p* = 0.022) compared to patients who were not (N = 119).

In univariable analysis, mean NAWM K2 coefficients were significantly associated with age, sex, body mass index (BMI), initial stroke severity as measured by admission National Institutes of Health Stroke Scale (NIHSS) score, mean ADC in NAWM, and contralateral WMHv (Tables 2 and 3). In a subset analysis of the thrombolysis group, we found that women still had significantly higher K2 coefficients than men (*p* = 0.0039) despite the smaller number of patients. However, this was no longer the case for non-thrombolysis group, where no statistically significant difference was found (*p* = 0.23). Correlation analysis among the thrombolysis group showed no significant correlation between K2 and the variables in Table 3. The opposite was true for the non-thrombolysis group, resulting in significant correlations for DWIv ( $\rho = 0.24$ , *p* = 0.0078), MTTv ( $\rho = 0.28$ , *p* = 0.0024), contralateral WMHv, ( $\rho = 0.24$ , *p* = 0.0081), ADC ( $\rho = 0.29$ , *p* = 0.0017), age ( $\rho = 0.35$ , *p* < 0.0001), NIHSS ( $\rho = 0.34$ , *p* = 0.0011), and baseline MMP-2 levels ( $\rho = 0.20$ , *p* = 0.0027).

Higher mean ADC in NAWM was significantly associated with hypertension (HTN), atrial fibrillation (AF), coronary artery disease (CAD), as well as age, systolic blood pressure (SBP), NIHSS, and K2 coefficients in NAWM (Tables 2 and 3). Both mean K2 and ADC in NAWM were correlated with elevated levels of MMP-2 at baseline, and mean ADC was correlated with MMP-2 levels at 48 h. MMP-2 levels at baseline (Spearman's  $\rho = 0.31$ , *p* < 0.0001) and at 48 h



**Table 1.** Clinical characteristics of the study population.

Demographics and risk factors	N = 184
Age, mean $\pm$ SD	68 $\pm$ 15
Female sex, n (%)	79 (43)
Caucasian, n (%)	177 (96)
Hispanic, n (%) <sup>a</sup>	11 (6)
Systolic blood pressure, <sup>b</sup> mean $\pm$ SD, mmHg	157 $\pm$ 28
Diastolic blood pressure, <sup>b</sup> mean $\pm$ SD, mmHg	84 $\pm$ 16
Creatinine, mean $\pm$ SD, mg/dL	1.04 $\pm$ 0.29
Body mass index, <sup>c</sup> kg/m <sup>2</sup>	28.1 $\pm$ 6.0
Admission NIHSS, median (IQR), points	5 (3–12)
Hypertension, n (%) <sup>a</sup>	129 (70)
Diabetes, n (%)	38 (21)
Atrial fibrillation, n (%)	50 (27)
Coronary artery disease, n (%)	44 (24)
Hyperlipidemia, n (%)	82 (45)
Prior stroke, n (%)	36 (20)
Smoking (current or past), n (%)	120 (65)
Thrombolytic treatment, n (%)	65 (35)
MMP-2 (Baseline), median [IQR], ng/mL	305 [238–370]
MMP-2 (48 h), <sup>d</sup> median [IQR], ng/mL	271 [220–338]
CCS classification, <sup>b</sup> n (%)	
Cardioembolic	94 (51)
Large artery atherosclerosis	39 (21)
Small vessel disease	9 (5)
Other	8 (4)
Undetermined	33 (18)
Hemorrhagic transformation, <sup>e</sup> n (%)	
None	134 (77)
Parenchymal hematoma	16 (9)
Hemorrhagic infarction	24 (14)
Infarct volume (DWI), median [IQR], cm <sup>3</sup>	7.4 [1.3–22.7]
Perfusion deficit volume (MTT), median [IQR], cm <sup>3</sup>	25.5 [6.0–80.7]
Contralateral WMH volume, median [IQR], cm <sup>3</sup>	1.78 [0.84–4.5]
K2 coefficients ( $\times 10^{-6}$ ) in NAWM, mean $\pm$ SD, s <sup>-1</sup>	836 $\pm$ 2019
ADC ( $\times 10^{-6}$ ) in NAWM, mean $\pm$ SD, mm <sup>2</sup> /s	797 $\pm$ 59
90-day mRS, <sup>f</sup> median [IQR]	1 [1–3]
Favorable outcome (90-day mRS < 2), <sup>f</sup> n (%)	84 (54)

<sup>a</sup>N = 181; <sup>b</sup>N = 183; <sup>c</sup>N = 164; <sup>d</sup>N = 139; <sup>e</sup>N = 174; <sup>f</sup>N = 156.

ADC: apparent diffusion coefficient; CCS: Causative Classification of Stroke; DWI: diffusion-weighted imaging; IQR: interquartile range; MMP-2: matrix metalloproteinase-2; mRS: modified Rankin Scale score; MTT: mean transit time; WMHV: white matter hyperintensity volume; NAWM: normal-appearing white matter; NIHSS: National Institutes of Health Stroke Scale; SD: standard deviation; WMH: white matter hyperintensity.

(Spearman's  $\rho = 0.23$ ,  $p = 0.0072$ ) were significantly correlated with WMHV. Subset analyses as a function of thrombolysis found results similar to the entire cohort with the exception of CAD, which were no longer significant, most likely due to reduced sample size. For the thrombolysis group, correlation analysis produced similar results, except for SBP, NIHSS and 48-h MMP-2 levels were no longer significantly correlated with ADC values. In contrast for the non-thrombolysis group, only SBP was no longer significantly correlated with mean ADC. Contralesional WMHV was an independent predictor of both mean K2 ( $\beta$  411,  $p = 0.0007$ ) and ADC ( $\beta$  9.5,  $p = 0.0056$ ) in NAWM.

### Acute cerebral tissue injury

Acute DWIv and MTTv were correlated with mean NAWM K2 (DWIv Spearman's  $\rho$  0.15,  $p = 0.04$  and MTTv Spearman's  $\rho$  0.21,  $p = 0.0035$ ), but not with mean ADC values in NAWM (Table 3).

### Hemorrhagic transformation

Patients who experienced HT had higher K2 coefficients than those who did not ( $1092 \pm 1143$  vs.  $729 \pm 2066$ ,  $p = 0.02$ ). In addition, treating HT as an ordinal variable (none = 0, hemorrhagic infarction = 1, parenchymal hematoma = 2), found a significant correlation between more severe HT and increasing K2 (Spearman's  $\rho$  0.18,  $p = 0.017$ ). In contrast, there was no difference in mean ADC values between patients with and without HT ( $793 \pm 59$  vs.  $800 \pm 59$ ,  $p = 0.59$ ), nor significant correlation with HT severity (Spearman's  $\rho - 0.05$ ,  $p = 0.49$ ). The only independent predictor of HT was DWIv ( $\beta - 0.35$ ,  $p = 0.0027$ ).

### Functional outcomes after stroke

Long-term functional outcome after stroke was associated with MRI markers of acute and chronic cerebrovascular injury (Table 4). Mean NAWM K2 coefficients (Spearman's  $\rho$  0.16,  $p = 0.04$ ) and mean NAWM ADC values (Spearman's  $\rho$  0.40,  $p < 0.0001$ ) were correlated with 90-day mRS. Patients with unfavorable outcomes (mRS  $\geq 2$ ) had greater BBB permeability in NAWM ( $1145 \pm 2574$  vs.  $615 \pm 1658 \times 10^{-6}$ ,  $p = 0.03$ ) and higher mean diffusivity values ( $816 \pm 64$  vs.  $777 \pm 46 \times 10^{-6}$  mm<sup>2</sup>/s,  $p < 0.0001$ ). Similarly, elevated levels of MMP-2 at baseline were associated with worse long-term outcome (Spearman's  $\rho$  0.17,  $p = 0.037$ ).

In a univariable analysis, admission NIHSS, contralesional ADC, and linear-log transformed DWIv (all  $p < 0.0001$ ), linear-log transformed MTTv ( $p = 0.0002$ ), use of thrombolysis ( $p = 0.002$ ); age ( $p = 0.0003$ );

**Table 2.** Comparison of mean K2 coefficients and mean ADC values in normal appearing white matter between patients with clinical characteristic present and those without.

	Mean K2 coefficient ( $\times 10^{-6}$ ) ( $\pm$ SD) in NAWM			Mean ADC ( $\times 10^{-6}$ ) ( $\pm$ SD) in NAWM		
	Characteristic present? (Y/N)			Characteristic present? (Y/N)		
	Yes	No	P	Yes	No	P
Female	1027 $\pm$ 1193	693 $\pm$ 2461	0.0062	804 $\pm$ 69	792 $\pm$ 49	0.19
Caucasian	811 $\pm$ 2015	1468 $\pm$ 2166	0.82	797 $\pm$ 59	786 $\pm$ 30	0.76
Hispanic	1042 $\pm$ 952	830 $\pm$ 2071	0.58	778 $\pm$ 57	798 $\pm$ 59	0.34
Hypertension	753 $\pm$ 1712	1032 $\pm$ 2609	0.98	806 $\pm$ 59	776 $\pm$ 52	0.0005
Diabetes	1076 $\pm$ 2153	774 $\pm$ 1985	0.71	805 $\pm$ 57	795 $\pm$ 59	0.28
Atrial fibrillation	787 $\pm$ 2137	855 $\pm$ 1981	0.35	828 $\pm$ 62	785 $\pm$ 53	<0.0001
Coronary artery disease	1012 $\pm$ 1392	781 $\pm$ 2180	0.57	815 $\pm$ 68	792 $\pm$ 54	0.037
Hyperlipidemia	1017 $\pm$ 2141	691 $\pm$ 1913	0.65	800 $\pm$ 51	794 $\pm$ 64	0.43
Prior stroke	1307 $\pm$ 2570	722 $\pm$ 1853	0.08	807 $\pm$ 62	795 $\pm$ 58	0.14
Smoking	940 $\pm$ 2184	642 $\pm$ 1665	0.87	794 $\pm$ 52	802 $\pm$ 69	0.99
Thrombolytic treatment	640 $\pm$ 1953	944 $\pm$ 2054	0.63	798 $\pm$ 55	796 $\pm$ 61	0.50
CCS classification			0.74 <sup>a</sup>			0.084 <sup>a</sup>
Cardioembolic	921 $\pm$ 2237	–		806 $\pm$ 68	–	
Large artery Atherosclerosis	881 $\pm$ 1924	–		778 $\pm$ 39	–	
Small vessel disease	746 $\pm$ 1276	–		816 $\pm$ 54	–	
Other	1388 $\pm$ 1285	–		779 $\pm$ 54	–	
Undetermined	450 $\pm$ 1825	–		793 $\pm$ 45	–	

<sup>a</sup>Tested with analysis of variance.

CCS: causative classification of stroke; mRS: modified Rankin Scale score; SD: standard deviation.

**Table 3.** Correlation between continuous clinical characteristics and mean K2 coefficients and mean ADC values in normal appearing white matter.

	Mean K2 coefficients ( $\times 10^{-6}$ ) in NAWM		Mean ADC ( $\times 10^{-6}$ ) in NAWM	
	Spearman's coefficient	P	Spearman's coefficient	P
DWI lesion volume	0.15	0.04	0.03	0.72
MTT lesion volume	0.21	0.0035	0.049	0.51
Contralateral WMH volume	0.19	0.010	0.51	<0.0001
Mean ADC in NAWM	0.23	0.0014	–	–
Age	0.26	0.0004	0.61	<0.0001
Systolic blood pressure	–0.004	0.96	0.17	0.024
Diastolic blood pressure	–0.10	0.17	0.05	0.47
Creatinine	–0.067	0.37	0.089	0.23
Body mass index	–0.21	0.0064	–0.054	0.52
NIHSS score	0.19	0.0099	0.21	0.0043
MMP-2 (Baseline), ng/mL	0.17	0.022	0.37	<0.0001
MMP-2 (48 h), ng/mL	0.084	0.32	0.32	0.0001

ADC: apparent diffusion coefficient; DWI: diffusion-weighted imaging; IQR: interquartile range; MMP-2: matrix metallo-proteinase 2; mRS: modified Rankin Scale score; MTT: mean transit time; NAWM: normal-appearing white matter; NIHSS: National Institutes of Health Stroke Scale; SD: standard deviation; WMH: white matter hyperintensity.

linear-log transformed WMHv ( $p=0.006$ ); AF ( $p=0.01$ ); linear-log transformed baseline MMP-2 levels ( $p=0.037$ ); and K2 values ( $p=0.04$ ) were associated with 90-day mRS score, but not gender, race,

ethnicity, etiological stroke subtype, admission SBP or diastolic blood pressure (DBP), BMI, HT, or linear-log transformed 48-h MMP-2 levels, or history of HTN, hyperlipidemia (HL), diabetes mellitus (DM),

**Table 4.** Correlation of imaging markers of acute and chronic cerebrovascular injury with clinical outcomes.

	90-day mRS (N = 156)	
	Spearman's $\rho$	P
Chronic injury markers		
Contralateral WMH volume, cm <sup>3</sup>	0.22	0.0063
K2 coefficients ( $\times 10^{-6}$ ) in NAWM, s <sup>-1</sup>	0.16	0.040
ADC in NAWM ( $\times 10^{-6}$ ), mm <sup>2</sup> /s	0.40	<0.0001
Acute injury markers		
Infarct (DWI) volume, cm <sup>3</sup>	0.34	<0.0001
Perfusion deficit (MTT) volume, cm <sup>3</sup>	0.29	0.0002

ADC: apparent diffusion coefficient; DWI: diffusion-weighted imaging; mRS: modified Rankin Scale score; MTT: mean transit time; NAWM: normal-appearing white matter; WMH: white matter hyperintensity.

CAD, or prior stroke (all  $p > 0.05$ ). A backward stepwise analysis of all variables with univariate  $p$ -value  $< 0.10$  [including NIHSS, ADC, ln DWIv, ln MTTv, thrombolysis, age, ln WMHv, AF, baseline MMP-2, K2, prior stroke ( $p = 0.06$ ), and BMI ( $p = 0.06$ )] was carried out in association with (a) 90-day mRS score and (b) favorable outcome (mRS  $< 2$ ).

From the multivariable regression analysis of 90-day mRS, initial stroke severity (as measured by admission NIHSS score), history of prior stroke, and loss of microstructural integrity of white matter in contralesional NAWM, as measured by ADC, emerged as independent predictors of long-term functional outcome after AIS (Table 5).

## Discussion

In this study, we report that in patients with AIS, increased BBB permeability is associated with (a) loss of microstructural NAWM integrity and (b) acute cerebral tissue and long-term functional outcomes. Our data demonstrate that post-stroke outcomes are less favorable in patients with pre-existing chronic microvascular dysfunction, as manifested by diffusely increased BBB permeability and loss of microstructural white matter integrity measured with perfusion- and diffusion-weighted MRI, respectively. This diffuse injury is detectable in the hemisphere putatively unaffected by acute ischemia, in the white matter that appears to be otherwise normal in conventional T2-weighted FLAIR images. This finding may help provide a pathophysiologic explanation for the long-observed association between pre-stroke functional status and post-stroke functional outcome.<sup>26–28</sup>

**Table 5.** Final predictors of 90-day functional outcome in 156 subjects with acute ischemic stroke.

	90-day mRS score: Final predictors	
	B	P
Admission NIHSS	0.13	<0.0001
ADC in NAWM	0.0059	0.002
Thrombolytic treatment (yes)	0.18	0.082
Prior stroke (no)	−0.35	0.0039
Age	0.013	0.068

ADC: apparent diffusion coefficient; NAWM: normal-appearing white matter; NIHSS: National Institutes of Health Stroke scale score; mRS: modified Rankin Scale score; TPA: tissue plasminogen activator.

Our results also identify elevated NAWM diffusivity and increased BBB permeability as imaging biomarkers that may be useful in providing individualized, patient-specific assessments of the effects of long-term vascular risk factor exposure, which has previously been linked to worse post-stroke outcomes.

Our study shows that WMH burden is an independent predictor of mean K2 coefficients in NAWM, a measure of diffuse BBB permeability. These data corroborate a recently reported increase in “BBB leakage” in patients with SVD,<sup>29</sup> and support the hypothesis that diffuse cerebral microvascular dysfunction is a common disease mechanism leading to both diffuse loss of BBB integrity and focal white matter lesions. We tested this hypothesis in a cohort of AIS patients undergoing acute clinical MRI with PWI, a population that is uniquely suited for this experiment, given their appreciable burden of WMH<sup>30</sup> and availability of a measurable outcome after an acute event. To avoid confounding by acute ischemic changes on MRI, we extracted the BBB permeability metrics from NAWM, and measured WMHv in the hemisphere contralateral to acute infarct. The association between NAWM K2 coefficients and WMHv in the contralesional hemisphere implies that the “leaky” BBB may, at least in part, contribute to pre-existing burden of leukoaraiosis, as suggested in a number of prior reports.<sup>8,31,32</sup>

We further validated this observation by testing the association between K2 coefficients and plasma levels of MMP-2, an enzyme widely regarded as contributory to chronic BBB remodeling, as a potential biological mechanism underlying diffuse cerebrovascular endothelial dysfunction, increased BBB permeability, and leading to microangiopathic white matter changes.<sup>33,34</sup> We observed a modest, albeit statistically significant correlation between mean K2 coefficients in NAWM and plasma MMP-2 levels within 9 h of LKW time, suggesting that this MMP-2 elevation reflects a chronic microangiopathic process injurious to white matter,

consistent with our findings reported in a larger cohort.<sup>12</sup> While other confounders related to stroke severity, stroke subtype, pre-existing and acute comorbidities, as well as medical interventions for stroke in the hyperacute phase might alter circulating levels of biomarkers,<sup>35,36</sup> and consequently, limit their utility in AIS, further studies of MMP-2 as a potential link to the “leaky BBB” and diseased white matter are warranted. MMP-2 has been extensively studied as a potential biomarker of many disorders including acute myocardial infarction,<sup>35</sup> although data are limited with regard to MMP-2 levels in acute stroke patients vs. non-stroke controls.<sup>36</sup> However, these studies of stroke and MMP-2 did not take into account severity of WMH, nor was the stroke-free status of controls verified using MRI. While we are unable to compare our results with the prior data directly, both baseline and 48-h MMP-2 levels in our AIS cohort were within the previously published range. Overall, this novel association between WMH burden and MMP-2 levels in AIS requires future study.

Another piece of evidence regarding the link between BBB permeability and white matter disease in our study is correlation, albeit modest, between NAWM K2 coefficients and ADC values, which is often interpreted as MRI markers of diffuse white matter structural integrity. A number of prior studies found that *microstructural* changes in NAWM precede *macrostructural* changes, that are ultimately visualized on T2 FLAIR MRI as WMH.<sup>37,29</sup> Using ADC to estimate diffusivity of the water molecules along white matter tracts allows us to quantify the degree of structural integrity of NAWM, which is known to represent the total burden of white matter disease in the brain exposed to long-term vascular risk factors.<sup>38</sup> In our study, mean K2 coefficients correlated positively with the elevated values of ADC in NAWM, implying that the BBB permeability is associated with greater microstructural damage of the white matter, and as such, serving as a marker of a potential underlying mechanism of disease that links cerebral microvascular dysfunction and WMH. Furthermore, despite its “normal appearance” on T2 FLAIR MRI, NAWM in patients with ischemic stroke might demonstrate early, albeit subclinical, changes that contribute to the overall burden of white matter injury due to diffuse microvascular changes and related disability.<sup>39,40</sup>

Whereas WMH severity was a strong predictor of both K2 and ADC values in NAWM, they correlated with different vascular risk factors. Higher mean NAWM K2 values were associated with age, female sex, and lower BMI, and mean ADC values in contralateral NAWM were associated with age, increased admission SBP and history of HTN, as well as CAD and AF. The differences between the vascular risk

profiles associated with NAWM K2 and ADC may highlight the distinct aspects of cerebrovascular disease captured by these imaging parameters and, possibly, point at the contributing mechanisms of disease. Specifically, microstructural integrity of the NAWM, as reflected in mean ADC, might be affected by life-long exposure to the common cardiovascular risk factors (HTN, CAD, AF) and is subject to their related pathophysiology.<sup>29,41,42</sup> However, the disease biology related to female sex-specific factors and relationship with BMI (i.e., the “obesity paradox”) in developing greater BBB permeability is likely more complex and requires further study.<sup>43,44</sup> The role of age in these disease processes remains to be fully understood; however, being the most important determinant of WMHv across any population ever studied, age was the only other predictor of mean NAWM ADC independent of WMHv in this cohort, implying that its role varies in cerebrovascular disease biology.<sup>29</sup> In addition, thrombolysis appeared to affect K2 coefficients more so than ADC. Females had significantly higher K2 coefficients than males only in the thrombolysis group, but not the non-thrombolysis group, despite smaller cohort size. In addition, in correlation analysis, many of the variables in Table 3 were no longer significantly correlated with K2 coefficients in the thrombolysis group. These results likely suggest an interaction between thrombolysis and BBB permeability, which is known to occur.

Finally, we report that the MRI metrics of microvascular dysfunction are associated with variables reflective of stroke severity, as well as ischemic tissue and clinical outcomes. In our study, elevated NAWM K2 and ADC values are correlated with higher admission NIHSS and worse functional outcomes at 90 days post-stroke. Furthermore, higher BBB permeability in NAWM was associated with greater DWI lesion size, increased volume of MTT perfusion deficit, and greater risk of HT at 48-h post-stroke. These data suggest that the pre-existing subclinical white matter injury may play a significant role in the brain microvascular compensatory capacity and susceptibility to acute ischemia. Diffusely increased permeability of the BBB may reflect up-regulation of pro-inflammatory cascade, increasing oxidative stress, and limited capacity of the brain tissue to counteract the effects of acute ischemia.<sup>1-3</sup> Because these chronic BBB changes are diffuse, acute-on-chronic injury during AIS in the affected area results in relatively larger infarct volumes and higher rate of HT of acutely infarcted tissue. The association of elevated NAWM K2 and ADC values with higher NIHSS may also suggest the role of pre-existing white matter integrity in mechanisms of early recovery during AIS.<sup>2</sup> Similarly, our findings uncover a correlation between unfavorable post-stroke functional outcome and the growing burden of cerebral white matter damage



accounted for by the (a) total volume of WMH, (b) microstructural injury as estimated by elevated mean diffusivity in NAWM, and (c) diffuse increase in the BBB permeability signaling endothelial dysfunction of the small cerebral vasculature. In this context, BBB disruption might appear as a tentative biological target for novel therapies aimed at mitigating brain injury and improving functional recovery after acute stroke.

This study has a number of important limitations. First, the retrospective study design and missing data points for several variables (including 28 missing points for 90-day mRS, 10 for HT, 19 for BMI, and 45 for 48-h MMP-2 levels) might have led to diminished statistical power of this analysis to demonstrate the extent of association with the MRI characteristics. As a result, the variables with missing data elements might have failed to emerge as independent predictors in multivariable models. This limitation is also important in consideration of potential confounders, such as reperfusion status after thrombolytic treatment or precise duration of stroke symptoms (time from LKW to MRI), which are not available in our dataset but could be related to imaging characteristics or clinical outcomes in this patient population. Secondly, a potential selection bias might exist in the hospital-based studies of AIS subjects with lower stroke severity and higher proportion of favorable outcomes, such as ours. However, this type of bias would underestimate the effect of association between the MRI measures and the metrics of outcome, including in multivariable models, i.e. increasing the chance of type II error. Third, this study is limited to AIS patients who underwent MRI with PWI within 9 h of LKW, and while the characteristics of our overall AIS cohort are consistent with those of average hospital-based AIS studies, we acknowledge that MRI-based studies are more likely to miss patients with milder (unrecognized) or more severe (too sick to undergo an MRI) stroke syndromes. A related limitation is the lack of baseline MRI data on the patients presenting with AIS and consequently, a question remaining as to whether acute ischemia may directly impact MRI measurements, such as mean K2 coefficient and ADC values. A recent study indicated that, at least, transient elevation of BBB permeability can be seen in the brain regions contralateral to acute stroke.<sup>45</sup> While findings of increased permeability in that report were limited by assessment of only a “mirror” stroke lesion ROI and inclusion of both grey and white matter permeability estimates in their analysis, a possibility of global BBB changes in the setting of acute ischemia warrants further consideration. Nevertheless, a transient global increase in BBB permeability during AIS does not explain the association between the degree of BBB leakiness and WMH burden, nor does it explain the link between WMH and

diffusivity metrics we observe in our dataset. Even if the BBB change is transient, our results suggest that patients with larger WMH burden are more likely to show greater increase in BBB permeability due to an already diffusely compromised microvasculature. Furthermore, our data align with the prior reports of association between the leaky BBB and loss of microstructural NAWM integrity in non-AIS subjects.<sup>14</sup> Prospective studies aiming to assess the MRI characteristics of WM integrity in stroke-free individuals, AIS patients, and convalescent stroke survivors could clarify this issue, and until then, current data should be interpreted with caution.

Another potential limitation is limited sensitivity of DSC perfusion imaging-derived K2 coefficients in measuring BBB changes, particularly in the setting of delayed bolus arrival and/or decreased blood flow. In fact, K2 coefficients in normal brain tissue such as NAWM are expected to be very low, as in our clinical dataset (mean NAWM K2 of  $836 \times 10^{-6} s^{-1}$ ). In addition, there are limited studies in regards to the reproducibility and repeatability of K2 values across patients and across scanners, as exists for other techniques that measure BBB permeability, such as dynamic contrast enhanced MRI (DCE) which measures Ktrans. There have been studies showing good repeatability of corrected CBV maps (which are based on K2 data).<sup>46</sup> In addition, there has been a study which showed good correlation between Ktrans and K2.<sup>47</sup> Clearly more research focused on the repeatability and reproducibility of K2 is needed. Some previous studies<sup>29,45</sup> have utilized DCE rather than DSC perfusion imaging, thereby possibly detecting changes in BBB permeability more accurately. However, DCE in the brain typically requires very long acquisition times (>20 min), which are not practical in acute stroke settings. MR perfusion imaging used in the context of clinical management of AIS patients typically includes DSC PWI based on its relatively short acquisition time, thereby rendering DCE imaging of limited use in the AIS clinical scenario. In addition, DSC is susceptible to a number of artifacts such as changes in T1 or T2, which may be present in stroke patients and which may lead to incorrect estimates of permeability. However, clinical MRI protocols used in AIS evaluation are extremely time-sensitive, and as a result, T1 and T2 mapping that may lead to more accurate characterization of permeability is typically not done in this patient population due to the extra time currently required to acquire this data. By limiting our analysis to the contralateral hemisphere, we sought to minimize potential confounds from delayed flow as well as from ischemic effects from the index stroke on K2 measures. Despite the limitations of DSC use for assessment of vascular permeability, we were able to

demonstrate associations between K2 coefficients and WMH burden, as well as functional outcome after stroke. This suggests that a pragmatic approach to BBB permeability measurement could include analysis of the DSC perfusion imaging.

A major strength of our study is inclusion of the largest-to-date cohort of AIS subjects with comprehensive, quantitative characterization of the NAWM using diffusion- and perfusion-derived metrics. In addition, we tested the potential role of MMP-2 as a biomarker of chronic BBB remodeling in association with MRI characteristics, as well as clinical and neuroimaging assessment of post-stroke outcomes. All MRI and laboratory variables in this analysis were collected by investigators blinded to clinical outcome, and the study was completed using standardized approach to data collection and quality control, as per SPOTRIAS criteria.<sup>12</sup>

In summary, our findings indicate that increased BBB permeability in NAWM of the contralesional hemisphere is associated with loss of white matter structural integrity and post-stroke outcomes. Furthermore, diffusivity metrics in NAWM are strongly associated with WMHv, which is consistent with its role as a marker of microstructural white matter disarray, likely related to dysregulation of chronic BBB remodeling, as evidenced by elevated MMP-2 levels. In the future, measuring these diffuse microangiopathic changes on MRI in patients with AIS may improve prediction of cerebral tissue and functional post-stroke outcomes.

### Funding

The author(s) disclosed receipt of the following financial support for the research, authorship, and/or publication of this article: This work was supported by the National Institutes of Health NINDS Specialized Program of Transitional Research in Acute Stroke (SPOTRIAS) grant P50-NS051343 (Furie PI); R01NS082285 (SALVO study, Rost PI); R01NS086905 (Rost, PI); R01NS059775 (Wu, PI); R01NS086905 (Wu, PI). Natalia Rost is supported in part by NIH-NINDS R01NS082285 & NS086905. Pedro Cougo was supported by NIH 5P50NS051343. Svetlana Lorenzano was supported by NIH 5P50NS051343. Hua Li was supported by NIH 5P50NS051343. Steven K Feske was supported by NIH 5P50NS051343. Karen L Furie was supported by NIH 5P50NS051343. Ona Wu is supported in part by NIH-NINDS P50NS051343, R01NS059775 and R01NS063925, R01NS082285 & NS086905. She is the co-inventor of a patent on "Delay-compensated calculation of tissue blood flow," US Patent 7,512,435, 31 March 2009, and the patent has been licensed to General Electric, Siemens, Imaging Biometrics and Olea Medical.

### Declaration of conflicting interests

The author(s) declared no potential conflicts of interest with respect to the research, authorship, and/or publication of this article.

### Authors' contributions

Natalia S Rost: study concept/design, study supervision, data acquisition, interpretation of data, drafting/revising the manuscript for intellectual content

Pedro Cougo: study design, data acquisition, statistical analysis/interpretation of data, drafting/revising the manuscript for intellectual content.

Svetlana Lorenzano: data acquisition, interpretation of data, drafting/revising the manuscript for intellectual content

Hua Li: data acquisition, revising the manuscript for intellectual content.

Lisa Cloonan: data acquisition, revising the manuscript for intellectual content.

Mark JR Bouts: data acquisition, revising the manuscript for intellectual content.

Arne Lauer: data acquisition, revising the manuscript for intellectual content.

Mark R Etherton: data acquisition, revising the manuscript for intellectual content.

Hasan H Karadeli: data acquisition, revising the manuscript for intellectual content.

Patricia L Musolino: interpretation of data, revising the manuscript for intellectual content.

William A Copen: interpretation of data, revising the manuscript for intellectual content.

Ken Arai: data acquisition, revising the manuscript for intellectual content.

Eng H Lo: data acquisition, revising the manuscript for intellectual content.

Steven K Feske: study design, study supervision, revising the manuscript for intellectual content.

Karen L Furie: study design, study supervision, revising the manuscript for intellectual content.

Ona Wu: study concept and design, data acquisition, data analysis and interpretation of data, drafting/revising the manuscript for intellectual content.

### References

1. Ay H, Arsava EM, Rosand J, et al. Severity of leukoaraiosis and susceptibility to infarct growth in acute stroke. *Stroke* 2008; 39: 1409–1413.
2. Rost NS, Fitzpatrick K, Biffi A, Kanakis A, et al. White matter hyperintensity burden and susceptibility to cerebral ischemia. *Stroke* 2010; 41: 2807–2811.
3. Arsava EM, Rahman R, Rosand J, et al. Severity of leukoaraiosis correlates with clinical outcome after ischemic stroke. *Neurology* 2009; 72: 1403–1410.
4. Pantoni L and Garcia JH. Pathogenesis of leukoaraiosis: a review. *Stroke* 1997; 28: 652–659.
5. O'Sullivan M, Lythgoe DJ, Pereira AC, et al. Patterns of cerebral blood flow reduction in patients with ischemic leukoaraiosis. *Neurology* 2002; 59: 321–326.
6. Isaka Y, Okamoto M, Ashida K, et al. Decreased cerebrovascular dilatatory capacity in subjects with asymptomatic periventricular hyperintensities. *Stroke* 1994; 25: 375–381.
7. Shi Y, Thrippleton MJ, Makin SD, et al. Cerebral blood flow in small vessel disease: a systematic review and meta-analysis. *J Cereb Blood Flow Metab* 2016; 36: 1653–1667.

8. Wardlaw JM, Doubal FN, Valdes-Hernandez M, et al. Blood-brain barrier permeability and long-term clinical and imaging outcomes in cerebral small vessel disease. *Stroke* 2013; 44: 525–527.
9. Wardlaw JM, Sandercock PA, Dennis MS, et al. Is breakdown of the blood-brain barrier responsible for lacunar stroke, leukoaraiosis, and dementia? *Stroke* 2003; 34: 806–812.
10. Chen C, Ostrowski RP, Zhou C, et al. Suppression of hypoxia-inducible factor-1 $\alpha$  and its downstream genes reduces acute hyperglycemia-enhanced hemorrhagic transformation in a rat model of cerebral ischemia. *J Neurosci Res* 2010; 88: 2046–2055.
11. Jalal FY, Yang Y, Thompson JF, et al. Hypoxia-induced neuroinflammatory white-matter injury reduced by minocycline in shr/sp. *J Cereb Blood Flow Metab* 2015; 35: 1145–1153.
12. Corbin ZA, Rost NS, Lorenzano S, et al. White matter hyperintensity volume correlates with matrix metalloproteinase-2 in acute ischemic stroke. *J Stroke Cerebrovasc Dis* 2014; 23: 1300–1306.
13. Boxerman JL, Schmainda KM and Weisskoff RM. Relative cerebral blood volume maps corrected for contrast agent extravasation significantly correlate with glioma tumor grade, whereas uncorrected maps do not. *AJNR* 2006; 27: 859–867.
14. Muñoz Maniega SCF, Valdés Hernández MC, Armitage PA, et al. Integrity of normal-appearing white matter: influence of age, visible lesion burden and hypertension in patients with small-vessel disease. *J Cereb Blood Flow Metab* 2017; 37: 644–656.
15. Sorensen AG, Wu O, Copen WA, et al. Human acute cerebral ischemia: detection of changes in water diffusion anisotropy by using mr imaging. *Radiology* 1999; 212: 785–792.
16. Wu O, Ostergaard L, Weisskoff RM, et al. Tracer arrival timing-insensitive technique for estimating flow in mr perfusion-weighted imaging using singular value decomposition with a block-circulant deconvolution matrix. *Magn Reson Med* 2003; 50: 164–174.
17. Copen WA, Deipolyi AR, Schaefer PW, et al. Exposing hidden truncation-related errors in acute stroke perfusion imaging. *AJNR* 2015; 36: 638–645.
18. Collins DL, Neelin P, Peters TM, et al. Automatic 3d intersubject registration of mr volumetric data in standardized talairach space. *J Comput Assist Tomogr* 1994; 18: 192–205.
19. Laboratory of Neuro Imaging. Icbm 452 t1 atlas. 2016;2007.
20. Laboratory of Neuro Imaging. Icbm probabilistic atlases. 2016;2008.
21. Mazziotta J, Toga A, Evans A, et al. A probabilistic atlas and reference system for the human brain: international consortium for brain mapping (icbm). *Philos Trans R Soc Lond B Biol Sci* 2001; 356: 1293–1322.
22. McConnell Brain Imaging Centre. Bic – the mcconnell brain imaging centre: home page. 2015;2006.
23. Bruno A, Shah N, Lin C, et al. Improving modified rankin scale assessment with a simplified questionnaire. *Stroke* 2010; 41: 1048–1050.
24. Hacke W, Kaste M, Bluhmki E, et al. Thrombolysis with alteplase 3 to 4.5 hours after acute ischemic stroke. *N Engl J Med* 2008; 359: 1317–1329.
25. Bishop CM. *Neural networks for pattern recognition*. New York: Oxford University Press Inc., 1995.
26. Sharma JC, Fletcher S and Vassallo M. Strokes in the elderly – higher acute and 3-month mortality – an explanation. *Cerebrovasc Dis* 1999; 9: 2–9.
27. Pohjasvaara T, Erkinjuntti T, Vataja R, et al. Comparison of stroke features and disability in daily life in patients with ischemic stroke aged 55 to 70 and 71 to 85 years. *Stroke* 1997; 28: 729–735.
28. Anderson C. Baseline measures and outcome predictions. *Neuroepidemiology* 1994; 13: 283–289.
29. Muñoz Maniega S, Chappell FM, Valdes Hernandez MC, et al. Integrity of normal-appearing white matter: influence of age, visible lesion burden and hypertension in patients with small-vessel disease. *J Cereb Blood Flow Metab* 2017; 37: 644–656.
30. Rost NS, Rahman R, Sonni S, et al. Determinants of white matter hyperintensity volume in patients with acute ischemic stroke. *J Stroke Cerebrovasc Dis* 2010; 19: 230–235.
31. Farrall AJ and Wardlaw JM. Blood-brain barrier: ageing and microvascular disease – systematic review and meta-analysis. *Neurobiol Aging* 2009; 30: 337–352.
32. Wardlaw JM, Doubal F, Armitage P, et al. Lacunar stroke is associated with diffuse blood-brain barrier dysfunction. *Ann Neurol* 2009; 65: 194–202.
33. Candelario-Jalil E, Yang Y and Rosenberg GA. Diverse roles of matrix metalloproteinases and tissue inhibitors of metalloproteinases in neuroinflammation and cerebral ischemia. *Neuroscience* 2009; 158: 983–994.
34. Candelario-Jalil E, Thompson J, Taheri S, et al. Matrix metalloproteinases are associated with increased blood-brain barrier opening in vascular cognitive impairment. *Stroke* 2011; 42: 1345–1350.
35. Kai H IH, Yasukawa H, Kai M, et al. Peripheral blood levels of matrix metalloproteinases-2 and -9 are elevated in patients with acute coronary syndromes. *J Am Coll Cardiol* 1998; 32: 368–372.
36. Kreisel SH SM, Reuter B, Senn E, et al. Mmp-2 concentrations in stroke according to etiology: adjusting for enzyme degradation in stored deep-frozen serum and other methodological pitfalls. *J Clin Neurosci* 2012; 19: 1564–1567.
37. de Groot M, Verhaaren BF, de Boer R, et al. Changes in normal-appearing white matter precede development of white matter lesions. *Stroke* 2013; 44: 1037–1042.
38. Vernooij MW, de Groot M, van der Lugt A, et al. White matter atrophy and lesion formation explain the loss of structural integrity of white matter in aging. *Neuroimage* 2008; 43: 470–477.
39. Verlinden VJ, van der Geest JN, de Groot M, et al. Structural and microstructural brain changes predict impairment in daily functioning. *Am J Med* 2014; 127: 1089–1096 e1082.
40. Sedaghat S, Cremers LG, de Groot M, et al. Lower microstructural integrity of brain white matter is related to higher mortality. *Neurology* 2016; 87: 927–934.

41. de Bruijn RF, Akoudad S, Cremers LG, et al. Determinants, mri correlates, and prognosis of mild cognitive impairment: the rotterdam study. *J Alzheimers Dis* 2014; 42(Suppl 3): S239–S249.
42. Staals J, Makin SD, Doubal FN, et al. Stroke subtype, vascular risk factors, and total mri brain small-vessel disease burden. *Neurology* 2014; 83: 1228–1234.
43. Driscoll I, Gaussoin SA, Wassertheil-Smoller S, et al. Obesity and structural brain integrity in older women: the women's health initiative magnetic resonance imaging study. *J Gerontol A Biol Sci Med Sci* 2016; 71: 1216–1222.
44. Kullmann S, Callaghan MF, Heni M, et al. Specific white matter tissue microstructure changes associated with obesity. *Neuroimage* 2016; 125: 36–44.
45. Villringer KSCB, Ostwaldt AC, Grittner U, et al. Dce-mri blood-brain barrier assessment in acute ischemic stroke. *Neurology* 2017; 88: 433–440.
46. Jafari-Khouzani K EK, Kalpathy-Cramer J, Bjørnerud A, et al. Repeatability of cerebral perfusion using dynamic susceptibility contrast mri in glioblastoma patients. *Transl Oncol* 2015; 8: 137–146.
47. Bonekamp D DK, Wiestler B, Wick W, et al. Association of overall survival in patients with newly diagnosed glioblastoma with contrast-enhanced perfusion mri: comparison of intraindividually matched t1- and t2 (\*)-based bolus techniques. *J Magn Reson Imaging* 2015; 42: 87–96.